# Effect of Voltage Distribution Among Three Electrodes on Microdischarge Characteristics in AC-PDP With Long Discharge Path

Jae Young Kim, Hyun Kim, Heung-Sik Tae, *Senior Member, IEEE*, Jeong Hyun Seo, and Seok-Hyun Lee

***Abstract*—The effect of the three-electrode voltage distribution on the microdischarge characteristics of an ac-PDP with a long discharge path (400 $\mu$m) is investigated. It is found that the auxiliary pulse applied to the address electrode, which participates in the trigger discharge, plays a key role in lowering the sustain voltage in the long discharge path by both providing the priming particles to generate the main discharge and accumulating more wall charges with the proper polarity to help the next discharge. In particular, the amplitude and width of the auxiliary pulse are very important parameters in a large sustain gap structure, as they are related to both the electron channeling that bridges the long discharge path and the accumulation of wall charges on the sustain electrodes. Thus, the effect of the width and amplitude of the auxiliary short pulse on the discharge characteristics, such as a low sustain voltage, the luminance, and luminous efficiency, are extensively investigated. As a result, the existence of a proper width and amplitude for the auxiliary pulse to lower the sustain voltage is observed, thereby also improving the luminous efficiency.**

***Index Terms*—Auxiliary short pulse applied to address electrode, large sustain gap, long discharge path, voltage distribution among three electrodes.**

## I. Introduction

IT IS WELL known that a longer discharge path improves the luminous efficiency [1], [2]. However, the firing and sustaining voltages required to produce a discharge increase in proportion to the length of the discharge path. Thus, if the firing and sustain voltages can be lowered for a long discharge path, the luminous efficiency is expected to improve. Yet, reducing the firing and sustain voltages in a three electrode-type PDP is very difficult without using an additional electrode [3]. In the current three electrode-type PDP cell with a long discharge path ($> 400$ $\mu$m), the discharge mechanism suggested by L. Weber is used to produce a discharge easily and efficiently for a long discharge path [4], [5]: the triggering discharge is initiated between one of the sustain electrodes and the address electrode prior to the main discharge between the two sustain electrodes, as the discharge path between the two sustain electrodes is too long. The initial discharge then extends toward the other sustain electrode along the address electrode, thereby triggering the main discharge between the two sustain electrodes with a long discharge path. Although inverted sustain waveforms have been used to lower the sustain voltage, where an MgO surface works as the cathode electrode at the initiation of the triggering discharge, the sustain voltage is still high (>250 V). Proper control of the wall charge distribution accumulating on the three electrodes could also contribute to lowering the sustain voltage in the case of a long discharge path, as the distribution of wall charges among the three electrodes strongly depends on the voltage distribution among the three electrodes. However, this idea has not received much attention.

Accordingly, this paper investigates the effect of the voltage distribution among the three electrodes on the microdischarge characteristics of an ac-PDP with a long discharge path (400$\mu$m). In particular, the effect of the auxiliary pulse applied to the address electrode on the microdischarge characteristics, including the lowering of the sustain voltage, is examined experimentally. It was reported that an auxiliary pulse applied to the address electrode during a sustain period was used to improve the luminous characteristics of PDP cells for a conventional small sustain gap structure ($< 100$ $\mu$m) [6], [7]. However, for a large sustain gap structure, the auxiliary pulse was applied to the address electrode so as to lower the high sustain voltage induced by a large sustain gap [8]. Thus, the effects of application of an auxiliary pulse to the address electrode can vary depending on the sustain gap length. Therefore, the effect of the auxiliary pulse applied to the address electrode (hereinafter called the auxiliary pulse) on the spatial distribution of the wall charges among the three electrodes is examined using a simulation tool.

## II. Experimental SetUP

### A. Cell Structure and Discharge Conditions for Long Discharge Path

Fig. 1 shows the discharge cell structure employed in this experiment, where the sustain gap was 400 $\mu$m, the sustain electrode (X or Y) width was 100 $\mu$m, the address electrode (Z) was 80 $\mu$m, and the height of the barrier rib was 125 $\mu$m. An MgO layer with a thickness of 5000 Å was deposited on the dielectric layer of the front panel, while red, green, and blue phosphor layers, consisting of $(\mathrm{Y,Gd})\mathrm{BO}_3$ : Eu, $(\mathrm{Zn,Mn})_2\mathrm{SiO4}$,

Manuscript received May 5, 2005; revised July 22, 2006. This work was supported in part by Brain Korea 21 (BK21).

J. Y. Kim, H. Kim, and H.-S. Tae are with the School of Electrical Engineering and Computer Science, Kyungpook National University, Daegu 702-701, Korea (e-mail: hstae@ee.knu.ac.kr).

J. H. Seo is with the Department of Electronics, Incheon University, Incheon 402-751, Korea.

S.-H. Lee is with the School of Electrical Engineering, Inha University, Incheon 402-751, Korea.

Color versions of Figs. 1, 5, and 8 are available online at http://ieeexplore.ieee.org.

Digital Object Identifier 10.1109/TPS.2006.887766

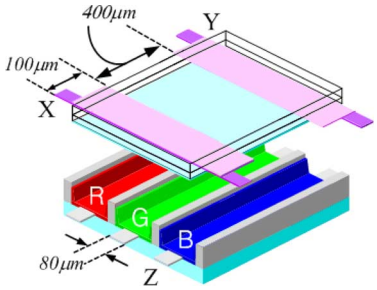


Fig. 1. Cell structure of test panel with long discharge path (400 $\mu$m) used in present study.

and (Ba, Eu)$MgAl_{10}O_{17}$, respectively, were deposited between the ribs on the rear panel. The gas pressure was 500 torr based on a mixture of Ne–Xe (5%). Fig. 2(a) shows the voltage threshold ($Vt$) close-curve measured from the cells of the test panel with a long discharge path in the case of no initial wall charges accumulated on the three electrodes. Unlike the typical $Vt$ close-curve showing a hexagon with six sides, the $Vt$ closed curve for the large sustain gap showed a parallelogram with only four sides, meaning that a discharge can not be directly produced between the X and Y electrodes due to the long distance between them. Thus, a surface discharge (X-Y discharge) can not be produced without first producing a face discharge (Z-Y or Z-X). Furthermore, the $Vt$ close-curve in Fig. 2(a) shows that the discharge initiation voltages for the Y-Z (or X-Z) discharge varied depending on whether the sustain electrode deposited with an MgO layer or the address electrode deposited with a phosphor layer worked as the cathode electrode. For the $Vt$ close-curve in Fig. 2(a), the applied voltage means the cell voltage, i.e., the firing voltage, as the $Vt$ close-curve was measured without any initial wall charges. As shown in the table in Fig. 2(b), the firing voltage difference between the MgO cathode and the phosphor cathode was about 70 V due to the higher secondary electron emission coefficient for the MgO cathode condition. Consequently, the MgO cathode condition produced an efficient trigger discharge for the main discharge.

Fig. 2(c) shows the specific voltage distribution necessary for an efficient sustain discharge with a long discharge path (400$\mu$m). To produce a trigger discharge between the X and Z electrodes with the MgO cathode condition prior to the main discharge, the cell voltage between the X and Z electrodes needs to be at least over the firing voltage for the MgO cathode condition (in this case, 188 V). When this condition is satisfied, a trigger discharge is initiated between the X and Z electrodes, thereby producing ions and electrons in the cell. If the electrons can then be attracted along the address electrode toward the Y electrode, the main discharge can be produced between the X and Y electrodes. To satisfy this condition, the potential at the Y electrode should be higher than that at the Z electrode. However, care should also be taken not to produce just a Y-Z discharge, that is, the potential difference between the Y and Z electrodes should be lower than the firing voltage for the phosphor cathode condition (in this case, 258 V). Since the discharge condition for a long discharge path requires a specific voltage distribution among the three electrodes, the potential variation of the Z electrode with respect to the X and Y electrodes is very important

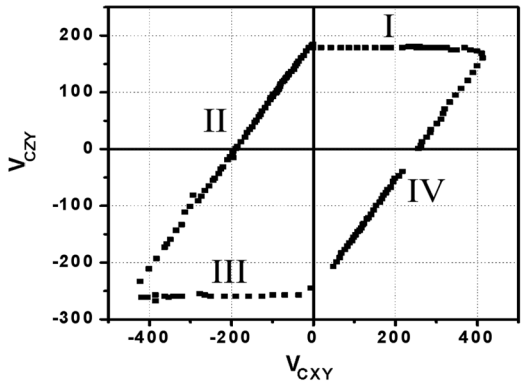


(a)

| Firing Condition | X-Z | Y-Z | Difference |
|---|---|---|---|
| MgO Cathode ($V_{f,\,MgO}$) | 188 V | 188 V | 70V |
| Phosphor Cathode ($V_{f,\,phosphor}$) | 258 V | 258V | |

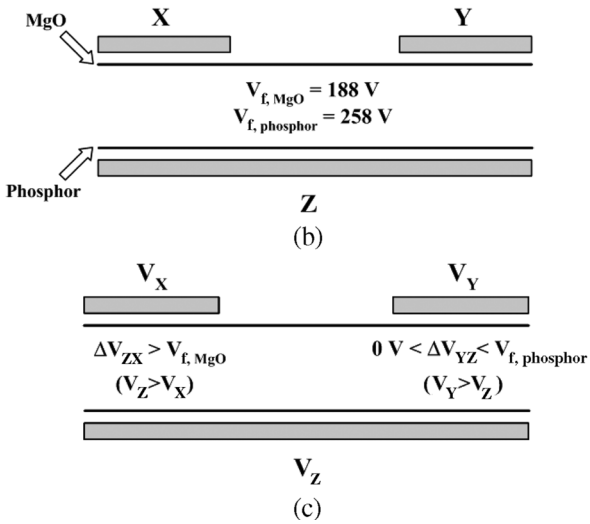


(b)

(c)

Fig. 2. (a) $Vt$ closed curve measured from cells of test panel with long discharge path and no initial wall charges accumulated on three electrodes, where I: $V_{tZY}$ = Discharge start threshold cell voltage between Z and Y; II: $V_{tZX}$ = Discharge start threshold cell voltage between Z and X; III: $V_{tYZ}$ = Discharge start threshold cell voltage between Y and Z; IV: $V_{tXZ}$ = Discharge start threshold cell voltage between X and Z. (b) Two different firing voltages obtained from measured $Vt$ close curve in (a), where $V_{f,\mathrm{MgO}}$ is firing voltage for MgO cathode condition and $V_{f,\mathrm{phosphor}}$ is firing voltage for phosphor cathode condition. (c) Specific voltage distribution required to produce efficient discharge with long discharge path.

for producing an efficient discharge in the case of a long discharge path.

### *B. Proposed Sustain Driving Waveforms and Sustainable Voltage Conditions for Long Discharge Path*

Fig. 3(a) shows the sustain driving waveforms used to produce a sustain discharge in the test panel with a long discharge path, where in case 1 no auxiliary pulse was applied to the address electrode, while in case 2 an auxiliary pulse was applied to the address electrode. The conventional sustain waveform shown in case 1 was unable to produce a discharge without applying a very high potential, as an X-Y discharge could not be produced directly due to the long discharge path. In general, a long discharge path tends to improve the discharge efficiency.

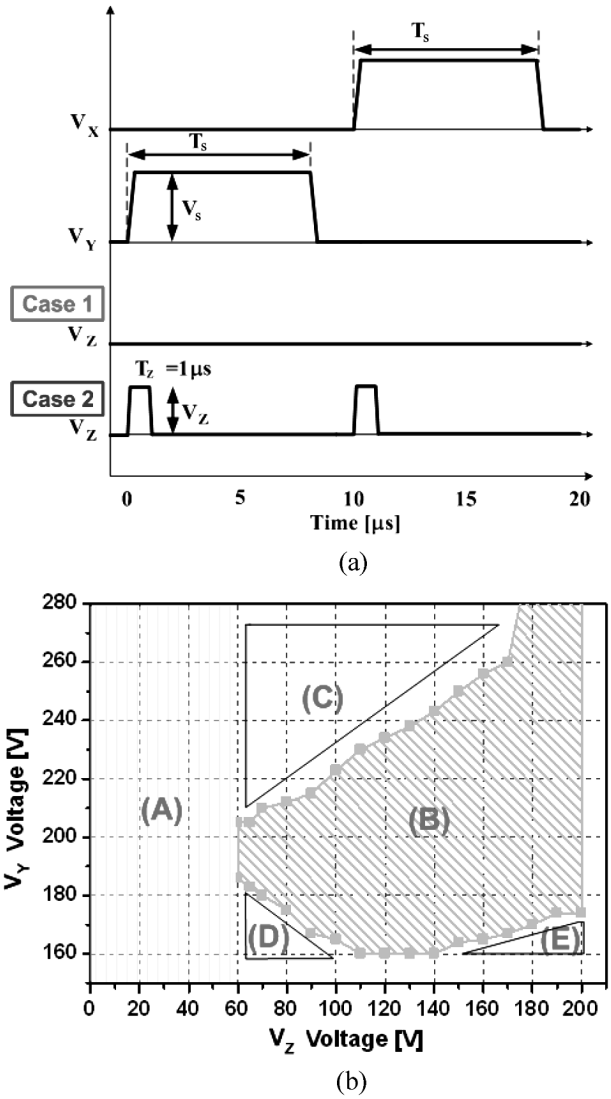


Fig. 3. (a) Driving waveforms for producing sustain discharge in test panel with long discharge path. Case 1: no auxiliary pulse is applied to address electrode. Case 2: auxiliary short pulse is applied to address electrode. (b) Sustainable voltage condition when applying case 2 sustain waveform in (a), where (B) is discharge region, and (A), (C), (D), and (E) are no discharge regions.

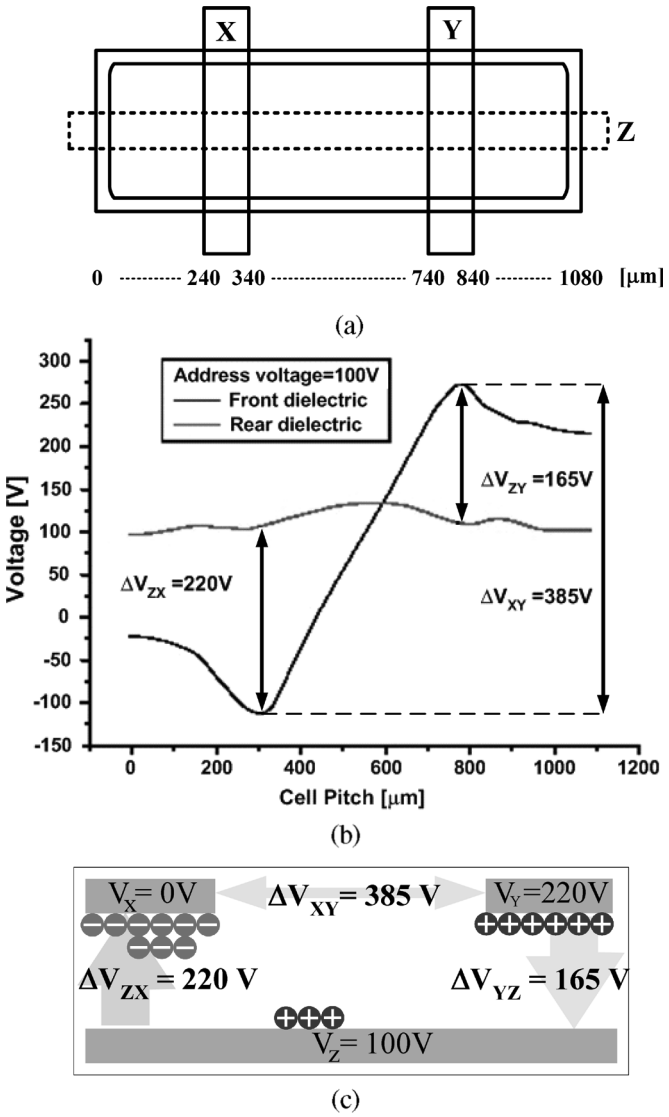


Fig. 4. (a) Schematic diagram of cell structure used in simulation. (b) Spatial voltage distribution on front surface and rear surface relative to cell position before discharge when applying case 2 driving waveform in Fig. 4(a), where $V_Y$ is 220 V and $V_Z$ is 100 V. (c) Diagram of wall voltage and applied voltage among three electrodes based on cell voltage obtained from simulation results in (b).

However, in a three electrode-type structure with a long discharge path, a discharge is produced between the sustain and address electrodes ahead of the main discharge between the two sustain electrodes, as the distance between the sustain and address electrodes is shorter than that between the two sustain electrodes. Consequently, even with a larger sustain gap, it is difficult to make the discharge path longer between the two sustain electrodes in the current three electrode-type PDP. Therefore, with a large sustain gap structure, it is important how to make a long electron trajectory efficiently, which involves controlling the potential at the address electrode that plays a role in channel bridging the two sustain electrodes. Thus, the case 2 sustain waveform in Fig. 3(a) is suggested, where a short pulse is also applied to the address electrode with the application of the sustain pulse to control the potential at the address electrode.

The potential difference between $V_X$ and $V_Z$ plus the wall voltage produces the trigger discharge between the X and Z electrodes with the MgO cathode condition. The resulting electrons then move along the Z electrode toward the Y electrode due to the positive potential $V_Y$, thereby bridging the X-Y discharge. In this driving method, the charged particles produced by the trigger discharge can be used as priming particles to promote an efficient main discharge. In the present experiment, the initial wall charges for the subsequent sustain discharge were made by applying the case 2 waveform in Fig. 3(a), where $V_Y$ was 300 V and $V_Z$ was 200 V, without adopting the reset and address waveforms. After the formation of the initial wall charges, the amplitude of the sustain pulse, $V_Y$ can be reduced if the amplitude and width of the auxiliary pulse, $V_Z$ are controlled properly.

Fig. 3(b) shows the sustainable voltage condition when applying the case 2 sustain waveform in Fig. 3(a). As shown, a long-gap discharge was only produced in region (B). Plus, no discharge was produced with either a zero $V_Z$ condition or low $V_X$ condition of less than 60 V, as shown in region (A), as the potential difference between the X and Z electrodes plus the wall

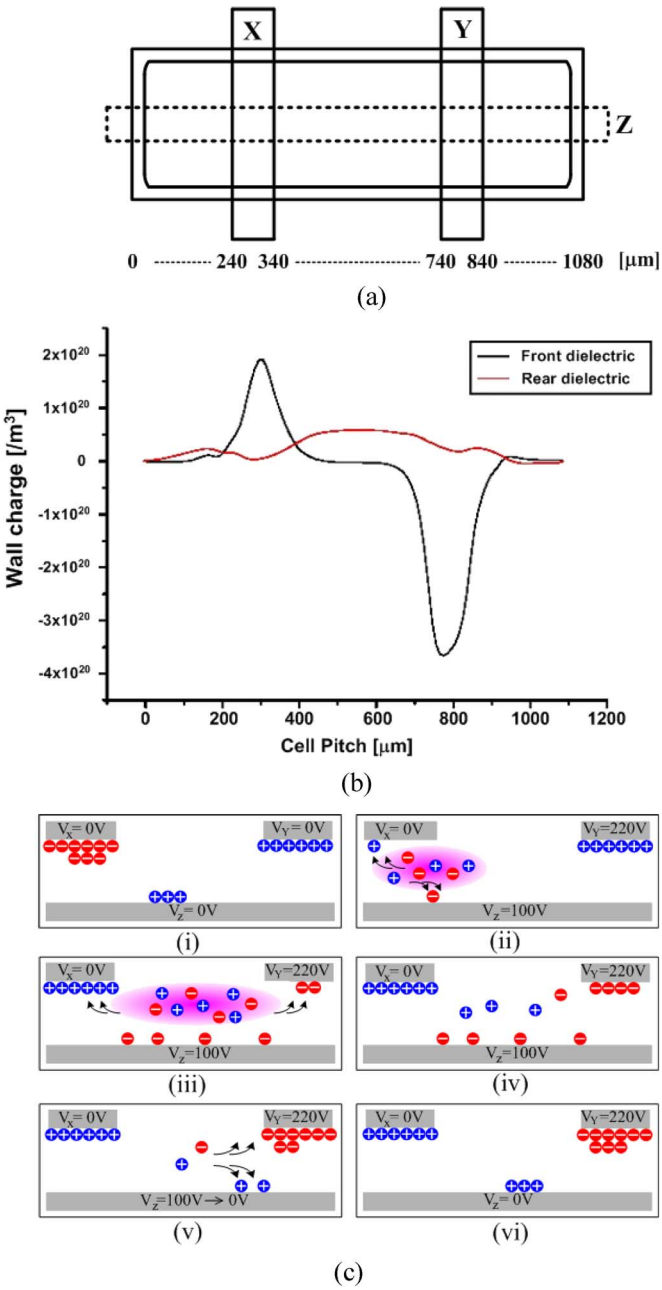


Fig. 5. (a) Schematic cell structure used in simulation. (b) Wall charge distribution on front surface and rear surface relative to cell position after discharge when applying case 2 driving waveform in Fig. 4(a), where $V_Y$ is 220 V and $V_Z$ is 100 V. (c) Diagram of wall charge distribution and applied voltage among three electrodes based on simulation results in (b).

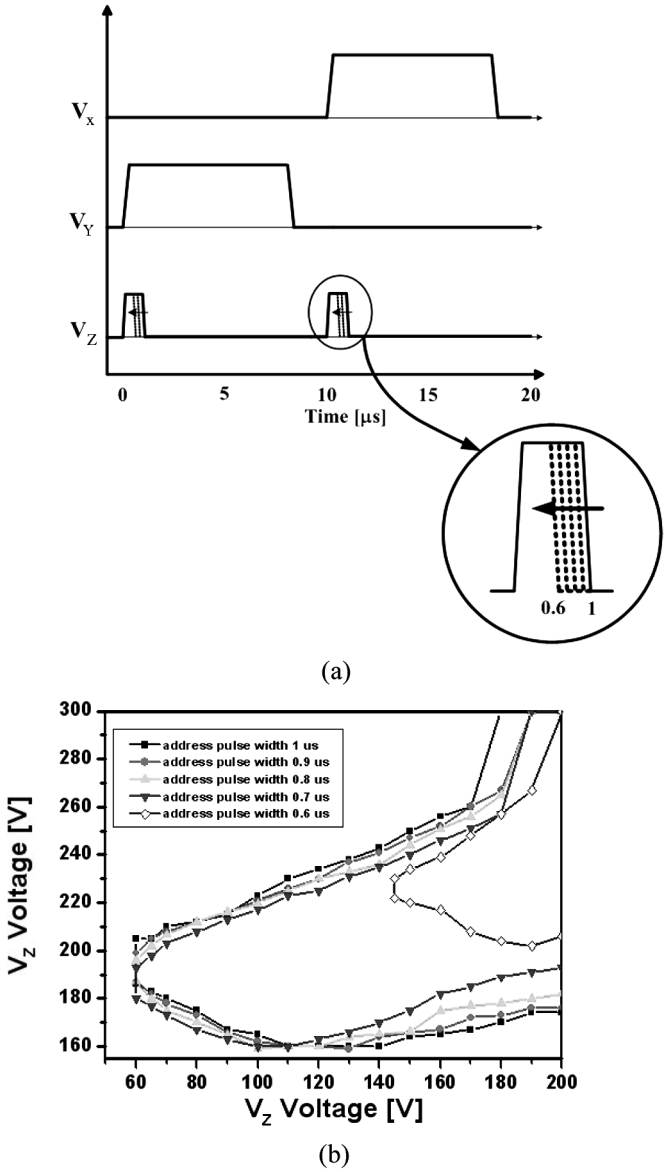


Fig. 6. (a) Voltage waveform with auxiliary short pulsewidth of less than 1 $\mu$s. (b) Sustainable voltage region.

voltage did not satisfy the firing voltage level necessary for a trigger discharge with the MgO cathode condition. When applying the auxiliary pulse, $V_Z$ with a proper value ranging from 60 to 200 V at a constant width of 1 $\mu$s, the sustain voltage, $V_Y$ was reduced to 160 V despite the long discharge path, as shown in (B) region, indicating that the elevated potential of the auxiliary electrode contributed to a low sustain voltage. The auxiliary pulse, $V_Z$ plays two roles in producing an efficient long-gap discharge, where the first is triggering the Z-X discharge, and the second is bridging the X-Y discharge using electron channeling along the Z electrode. However, the fulfillment of these two roles requires precise control of the amplitude and width of the auxiliary pulse, $V_Z$ with respect to the sustain pulse, $V_Y$. If the sustain voltage, $V_Y$ is too much higher than the auxiliary voltage, $V_Z$, as shown in region (C), no discharge is produced, as an independent discharge is produced between the Y and Z electrodes, and no electron channeling is formed along the Z electrode. Furthermore, as shown in regions (D) and (E), no discharge was produced when either $V_Z$ was higher than $V_Y$ (E) or $V_Y$ and $V_Z$ were both low (D).

## III. Simulation Results and Discussion

To investigate the effect of an auxiliary address pulse on the spatial voltage distribution in a three electrode-type structure with a long discharge path, a numerical analysis using a two-dimensional fluid model was applied [9], including Poisson, continuity, and drift-diffusion equations [10]. It was assumed that the local field approximation, i.e., the ionization and excitation

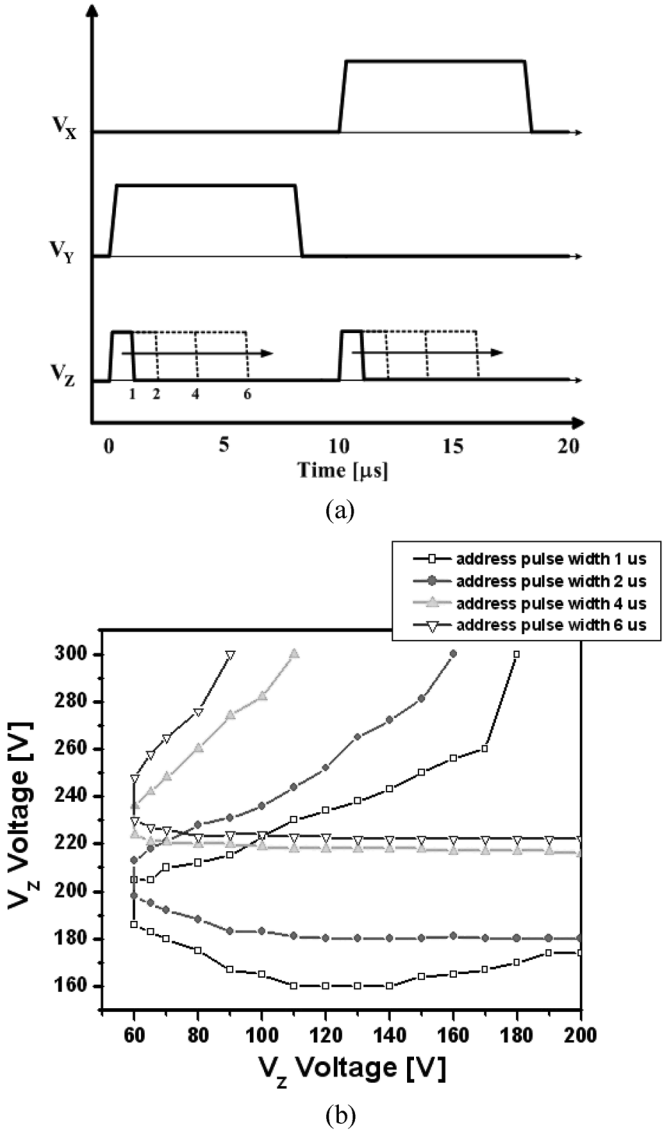


Fig. 7. (a) Voltage waveform with auxiliary short pulsewidth of over 1 $\mu$s. (b) Sustainable voltage region.

rates, were functions of the local field [11]. The reaction model consisted of 8 levels for Xe and 6 levels for Ne, plus the secondary electron coefficient $(\gamma)$ was assumed to be 0.2 for the Ne ions and 0.02 for the Xe ions. The cell used in this model was a conventional surface-type ac PDP with a long discharge path of 400 $\mu$m, as shown in the schematic cell structure of Fig. 4(a). Fig. 4(b) shows the simulation results for the voltage distribution on the surfaces of the front and rear dielectric layers relative to the cell position before the discharge when applying the case 2 driving waveform in Fig. 3(a), where $V_Y$ was 220 V and $V_Z$ was 100 V. Fig. 4(c) then shows a diagram of the wall voltage and applied voltage among the three electrodes based on the cell voltage obtained by the simulation results in Fig. 4(b). In Fig. 4(b), $\Delta V_{ZX}$ means the cell voltage between the X and Z electrodes, representing the sum of the applied voltage $(V_a)$ and the wall voltage $(V_w)$ between the X and Z electrodes, whereas $\Delta V_{ZY}$ means the cell voltage between the Y and Z electrodes, representing the sum of the applied voltage $(V_a)$ and the wall voltage $(V_w)$ between the Y and Z electrodes. The simulation results prior to the discharge confirmed that the cell voltage $\Delta V_{ZX}(= 220\,V > V_{f,\mathrm{MgO}} = 188\,V)$ between the X and Z electrodes was high enough to produce a trigger discharge, while the cell voltage $\Delta V_{ZY}(= 165\,V < V_{f,\mathrm{phosphor}} = 258\,V)$ between the Y and Z electrodes was adequate enough to attract the electrons produced by the trigger discharge toward the Y electrode without producing a Y-Z discharge, even with the application of a low $V_Z(= 100\,V)$ to the Z electrode. These results also confirmed that the spatial wall charges were well distributed due to the application of the auxiliary pulse to the Z electrode, thereby satisfying the above discharge condition.

Fig. 5(b) shows the simulation results for the wall charge distribution after the discharge relative to the cell position when applying the case 2 driving waveform in Fig. 3(a), where $V_Y$ was 220 V and $V_Z$ was 100 V. Fig. 5(c) then shows a diagram of the temporal behavior of the wall charges among the three electrodes prior to and after the discharge based on the simulation results in Figs. 4(b) and 5(b). The results in Fig. 5(b) show that after the discharge, the positive wall charges were accumulated on the X electrode, while the negative wall charges were accumulated on the Y electrode. Plus, the positive wall charges were accumulated in the intermediate region of the address electrode. The positive wall charges accumulated on the X electrode and negative wall charges accumulated on the Y electrode both resulted from the application of the case 2 sustain waveform in Fig. 3(a) to the three electrodes, especially the application of the auxiliary address pulse to the address electrode. The spatial wall charge distribution also provides very important information as regards analyzing the function of the auxiliary pulse for producing an efficient long-gap discharge. The potential difference between the X and Z electrodes induced by the application of the positive auxiliary pulse to the Z electrode caused the ions produced by the trigger discharge to be attracted toward the X electrode, resulting in the positive wall charges being accumulated on the X electrode, as shown in (ii), (iii), and (iv) of Fig. 5(c). These accumulated positive wall charges then contributed to attracting the electrons along the address electrode in the next main discharge between the X and Y electrodes, thereby lowering the sustain voltage. Meanwhile, the sudden charge in the auxiliary pulse from 100 to 0 V after about 1 $\mu$s promoted the conversion of the space charges into negative wall charges due to the abrupt increase in the potential difference between the Y and Z electrodes, resulting in the accumulation of more negative wall charges on the Y electrode, as shown in (v) and (vi) of Fig. 5(c). These accumulated negative wall charges then contributed to the efficient production of the next trigger discharge with the application of a low auxiliary voltage.

## IV. Experimental Results and Discussion

### *A. Sustainable Voltage Region Relative to Width of Auxiliary Address Pulse*

The auxiliary pulse that participates in the trigger discharge plays a key role in producing the discharge with a long discharge path. As shown in Fig. 3(b), only an auxiliary pulse amplitude greater than 60 V contributed to producing the discharge, confirming that the amplitude of the auxiliary pulse plus the wall

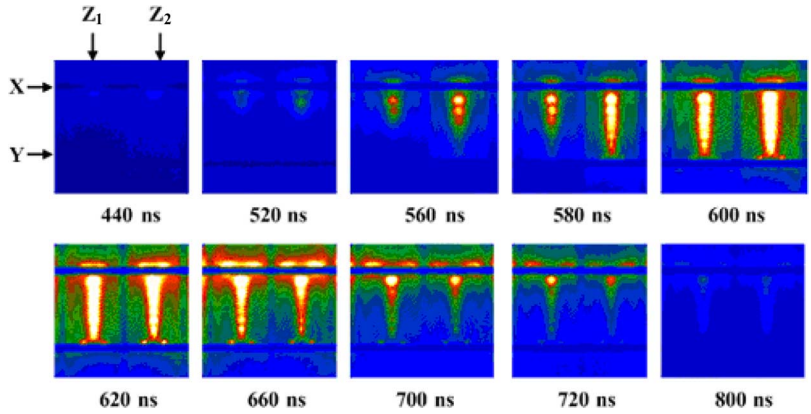


Fig. 8. IR emission images of discharge produced between two sustain electrodes with large sustain gap measured using gate mode condition of ICCD camera, where driving conditions for case 2 in Fig. 3(a) are as follows: $V_X$ is 0 V, $V_Y$ is 170 V, $V_Z$ is 90 V, and $T_Z$ is 1 $\mu$s.

voltage needed to be greater than the firing voltage to produce the trigger discharge, as mentioned in Fig. 4(c).

Figs. 6 and 7 show the changes in the sustainable voltage region with a variation in the width of the auxiliary short pulse. When the width decreased to 0.6 $\mu$s, the sustainable voltage region abruptly and significantly shrank, as shown in Fig. 6(b), indicating that an adequate time was required for the electron channeling along the address electrode to bridge the long discharge path. In other words, the positive polarity of the auxiliary pulse, $V_Z$ needed to be maintained until the main X-Y discharge was terminated. When the width of the auxiliary short pulse was shorter than 0.6 $\mu$s, it was observed that no discharge was produced. Furthermore, Fig. 7(b) shows that the minimum sustain voltage increased in proportion to an increase in the address pulsewidth over 1 $\mu$s, implying an optimal width condition for the auxiliary pulse, $V_Z$, to produce a large-gap discharge with a low sustain voltage.

### *B. ICCD Observation, IR Emission, and Discharge Current*

Fig. 8 shows IR emission images of the discharge produced between the two sustain electrodes with a large sustain gap (400 $\mu$m), measured using the gate mode condition of an ICCD camera where the driving conditions for case 2 in Fig. 3(a) were as follows: $V_X$ was 0 V, $V_Y$ was 170 V, the width of $V_Y(=T_Y)$ was 8 $\mu$s, $V_Z$ was 90 V, and the width of $V_Z(=T_Z)$ was 1$\mu$s. As shown in Fig. 8, the trigger discharge was initiated at 440 ns between the Z and X electrodes, then spread toward the opposite sustain electrode. The ICCD images illustrate that the duration of the main discharge between the X and Y electrodes was about 80 ns from 580 to 660 ns, plus the narrow shape of the main discharge was completely terminated at 800 ns, indicating that the width of the auxiliary pulse needed to be at least 0.7 $\mu$s. As such, when the polarity of the address pulse, $V_Z$, was abruptly changed from positive to ground prior to the extinction of the X-Y main discharge (i.e., the width of the address pulse was shorter than 0.7 $\mu$s), the main X-Y discharge was significantly disturbed or perturbed, resulting in an unstable large-gap discharge. This explains the big difference between 0.6 and 0.7 $\mu$s for the address pulsewidth with the proposed driving waveform, as shown in Fig. 6(b).

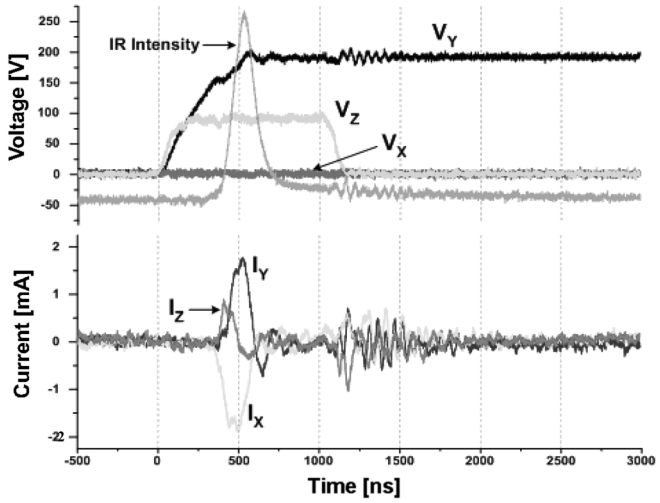


(a)

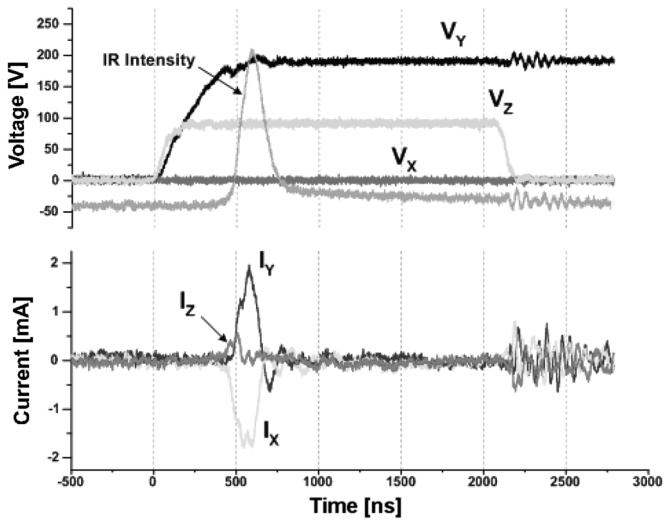


(b)

Fig. 9. Infrared (IR: 828 nm) emission waveform and discharge current waveforms flowing through three electrodes measured from 7-in. test panel, where driving conditions are (a) $V_Y$ is 190 V, $V_X$ is 0 V, $V_Z$ is 90 V, and width of $V_Z$ is 1 $\mu$s, and (b) $V_Y$ is 190 V, $V_X$ is 0 V, $V_Z$ is 90 V, and width of $V_Z$ is 2 $\mu$s.

The ICCD images in Fig. 8 showed a little different emission patterns in the two electrodes of $Z_1$ and $Z_2$ because they would

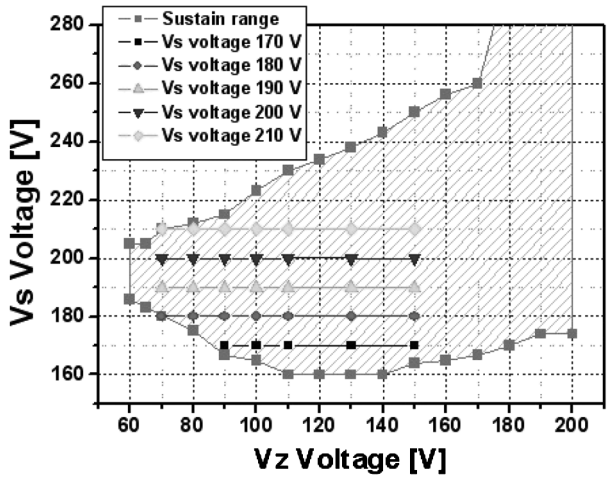


(a)

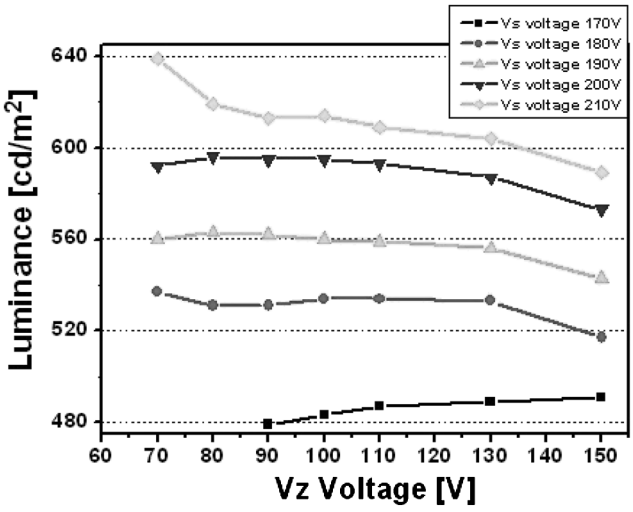


(b)

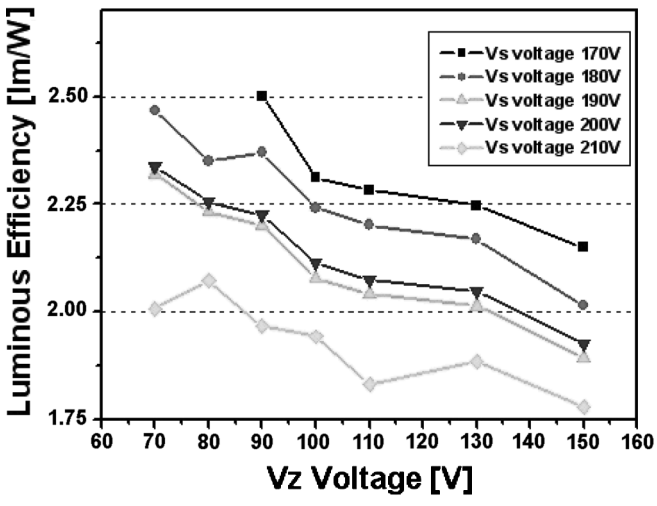


(c)

Fig. 10. (a) Changes in $V_Z$ at constant $V_X$ within sustain voltage region. (b) Luminance relative to $V_Z$ at various sustain voltages. (c) Luminous efficiency relative to $V_Z$ at various sustain voltages.

have a different phosphor condition ($Z_1$: green, and $Z_2$: blue). Due to the different phosphor layers in the two adjacent cells, the wall charges accumulated on the three electrodes could be slightly different. As a result, the time required for producing the trigger and main discharges could be different.

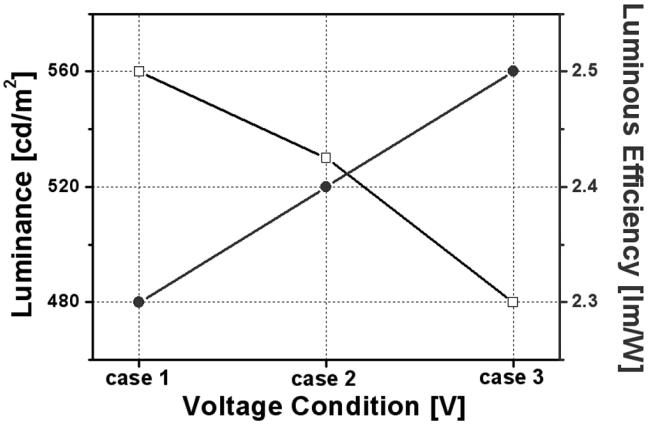


Fig. 11. Luminance and luminous efficiency with three different voltage distribution. Case 1: $V_Y = 190\ V$, $T_Y = 8\ \mu$s, $V_Z = 70\ V$, $T_Z = 1\ \mu$s. Case 2: $V_Y = 180\ V$, $T_Y = 8\ \mu$s, $V_Z = 80\ V$, $T_Z = 1\ \mu$s. Case 3: $V_Y = 170\ V$, $T_Y = 8\ \mu$s, $V_Z = 90\ V$, $T_Z = 1\ \mu$s.

Fig. 9(a) and (b) shows the infrared (IR: 828 nm) emission waveform and corresponding discharge current waveforms flowing through the three electrodes measured from the 7-in. test panel when the driving conditions were: (a) $V_Y$ was 190 V, $T_Y$ was 8 $\mu$s, $V_X$ was 0 V, $V_Z$ was 90 V, and $T_Z$ was 1 $\mu$s and (b) $V_Y$ was 190 V, $T_Y$ was 8 $\mu$s, $V_X$ was 0 V, $V_Z$ was 90 V, and $T_Z$ was 2 $\mu$s. As shown in Fig. 9, when the width of the auxiliary pulse, $V_Z$ was greater than 1 $\mu$s, the trigger discharge initiation was delayed and its intensity also diminished, even though the amplitudes of $V_Y$ and $V_Z$ were the same for both cases. This phenomenon may have been related to the change in the amount of wall charges accumulating on the three electrodes caused by the rapid change in the auxiliary pulse, $V_Z$ from positive to ground on the Z electrode after the extinction of the main X-Y discharge. Since many space charges still remained in the cell after the extinction of the main X-Y discharge, when the potential difference among the three electrodes within the cell was abruptly changed, this facilitated additional conversion of the space charges into wall charges. As a result, the amount of wall charges accumulated from the space charges increased in proportion to how the potential change of the auxiliary pulse from positive to ground coincided with the extinction of the main X-Y discharge. The increase in the wall charges accumulated on the X and Y sustain electrodes then contributed to lowering the sustain voltage required to produce the large-gap discharge. Conversely, delaying the potential change of the auxiliary pulse from positive to ground after the extinction of the main X-Y discharge caused a reduction in the amount of wall charges accumulated from the space charges, thereby increasing the sustain voltage required for the large-gap discharge. Therefore, the results in Fig. 9(b) indicate that a higher sustain voltage was needed to maintain the large-gap discharge when the width of the auxiliary pulse, $V_Z$ was greater than 1 $\mu$s.

### C. Luminance and Luminous Efficiency

To investigate the effect of the auxiliary pulse amplitude on the luminance and luminous efficiency, the amplitude of the

auxiliary pulse was increased in the case of a constant sustain voltage $V_S$ within the sustainable voltage region using an auxiliary pulsewidth of 1 $\mu$s, as shown in Fig. 10(a). In the case of a constant sustain voltage $V_S$, the luminance was hardly dependent on $V_Z$, whereas with a constant voltage for $V_Z$, the luminance increased with the sustain voltage $V_S$, as shown in Fig. 10(b). However, the luminous efficiency increased with a decrease in both the sustain and auxiliary voltages, $V_S$ and $V_Z$, as shown in Fig. 10(c). Thus, with an auxiliary pulsewidth of 1$\mu$s, a high luminous efficiency of 2.5 lm/W was obtained when $V_Z = 90\ V$ and $V_S = 170\ V$. Furthermore, the experimental data of Fig. 10(c) led us to estimate that the luminous efficiency in the long gap structure was improved by about 5–6% when the sustain voltage was reduced by 10 V.

Fig. 11 shows the luminance and luminous efficiency in the case of three different voltage distributions, where case 1 was $V_Y = 190\ V, T_Y = 8\ \mu$s, $V_Z = 70\ V, T_Z = 1\ \mu$s, case 2 was $V_Y = 180\ V, T_Y = 8\ \mu$s, $V_Z = 80\ V, T_Z = 1\ \mu$s, and case 3 was $V_Y = 170\ V, T_Y = 8\ \mu$s, $V_Z = 90\ V, T_Z = 1\ \mu$s. In all three cases, $V_S$ plus $V_Z$ was 260 V, nonetheless, the corresponding luminance and luminous efficiency varied depending on the $V_S$ and $V_Z$ combinations. The combination of a high $V_S$ and low $V_Z$ produced a high luminance and low luminous efficiency, whereas the combination of a low $V_S$ and high $V_Z$ produced a low luminance and high luminous efficiency. Therefore, these results indicate that lowering the sustain voltage was an essential factor for improving the luminous efficiency with a long discharge path. The effects of the pressure on the large sustain gap discharge has not been examined in this study. From a viewpoint of pd scaling in the plasma physics, the gas pressure can be lowered as the plasma dimension is lager, which means that the gas pressure of 500 torr used in this experiment would not be optimal especially in the large coplanar gap structure of 400$\mu$m. The relation between the pressure and the large sustain gap discharge needs to be examined carefully.

## V. Conclusion

The effect of the three-electrode voltage distribution on the microdischarge characteristics of an ac-PDP with a long discharge path (400 $\mu$m) was investigated. Numerical and experimental analyses revealed that the sustainable voltage region strongly depends on the width of the auxiliary pulse applied to the address electrode, and that the amplitudes of the sustain pulse $V_S$ and auxiliary pulse $V_z$ affect the luminance and luminous efficiency of a long-gap discharge.

## References


[1] J. D. Schemerhorn *et al.*, "A controlled lateral volume discharge for high luminous efficiency AC-PDP," in *Proc. SID Dig.*, 2000, pp. 106–109.

[2] J. T. Ouayng, Th. Callegari, B. Caillier, and J.-P. Boeuf, "Large gap plasma display cell with auxiliary electrode: Macro-cell experiment and two-dimensional modeling," *J. Phys. D: Appl. Phys.*, vol. 36, pp. 1959–1966, 2003.

[3] S. H. Lee, J. H. Lee, K. S. Lee, B. J. Shin, and K. C. Choi, "Improvement of the discharge time lag and luminous efficiency in an ac-PDP with 200 $\mu$m sustain gap," in *Pro. SID'04 Digest*, 2004, pp. 92–95.

[4] L. F. Weber, "Positive Column AC Display," U.S. Patent 6 184 848B1, Feb. 6, 2001.

[5] P. J. Drallos and L. F. Weber, "Simulations of ac PDP positive column and cathode fall efficiencies," in *Proc. IDRC'03 Dig.*, 2003, pp. 304–306.

[6] S. H. Jang, K.-D. Cho, H.-S. Tae, B. C. Choi, and K. C. Choi, "Inmprovement of luminous efficiency using address voltage pulse during sustain0period of ac-PDP," in *Proc. IDW'00*, 2000, pp. 767–770.

[7] K. Yamamoto, H. Kajiyama, K. Suzuki, S. Ho, and Y. Kawanami, "An address-voltage-modulation drive fir high-luminous-efficiency ac-PDPs," in *Proc. SID'02 Dig.*, 2002, pp. 856–859.

[8] H. Kim, H.-S. Tae, and S. I. Chien, "Long gap discharge characteristics based on control of voltage distribution among three electrodes for positive column ac-PDPs," in *Proc. SID'03 Dig.*, 2003, pp. 40–43.

[9] J. H. Seo, W. J. Chung, C. K. Yoon, J. K. Kim, and K. W. Whang, "Two-dimensional modeling of a surface type alternating current plasma display panel cell: Discharge dynamics and address voltage effects," *IEEE Trans. Plasma Sci.*, vol. 29, no. 5, p. 824, 2001.

[10] H. C. Kim, M. S. Hur, S. S. Yang, S. W. Shin, and J. K. Lee, "Three-dimensional fluid simulation of a plasma display panel cell," *J. Appl. Phys.*, vol. 91, pp. 9513–9520, 2002.

[11] J. Meunier, P. Belenguer, and J. B. Boeuf, "Numerical model of an ac plasma display panel cell in neon-xenon mixture," *J. Appl. Phys.*, vol. 78, pp. 731–745, 1995.

[12] H.-S. Tae, J.-W. Han, B.-G. Cho, and S.-I. Chien, "Temporal image sticking phenomena and reducing methods in AC PDP," in *Proc. IMID'04 Dig.*, 2004, pp. 176–179.


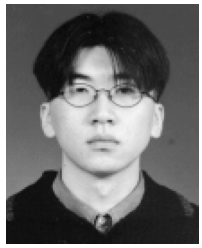

**Jae Young Kim** received the B.S. and M.S. degrees in electronic and electrical engineering from Kyungpook National University, Daegu, Korea, in 2002 and 2004, respectively, where he is currently pursuing the Ph.D. degree in electronic engineering.

His current research interests include plasma and microdischarge physics for plasma display applications.

**Hyun Kim** received the B.S. and M.S. degrees in electronic and electrical engineering from Kyungpook National University, Daegu, Korea, in 1999 and 2002, respectively, where he is currently pursuing the Ph.D. degree in electronic engineering.

He is also an Assistant Manager with CTO Display 2 Team, Samsung SDI Company Ltd., Yongin City, Korea.

**Heung-Sik Tae** (M'00–SM'05) received the B.S., M.S., and Ph.D. degrees in electrical engineering from Seoul National University, Seoul, Korea, in 1986, 1988, and 1994, respectively.

Since 1995, he has been a Professor in the School of Electrical Engineering and Computer Science, Kyungpook National University, Daegu, Korea. His research interests include the optical characterization and driving circuit of plasma display panels (PDPs), the design of millimeter wave guiding structures, and electromagnetic wave propagation using meta-material.

Dr. Tae is a member of the Society for Information Display (SID). He has been serving as an Editor for the IEEE Transactions on Electron Devices section on flat panel display since 2005.

**Jeong Hyun Seo** received the B.S. degree in electrical engineering in 1993 and the M.S. and Ph.D. degrees in plasma engineering in 1995 and 2000, respectively, all from Seoul National University, Seoul, Korea.

He was with the PDP Division, Samsung SDI, Chonan, Korea, from 2000 to 2002, where his work focused on the design of driving pulses in AC PDP. Since September 2002, he has been a Professor in the Department of Electronics Engineering, University of Incheon, Incheon, Korea.

**Seok-Hyun Lee** received the B.S. degree in electrical engineering in 1985 and the M.S. and Ph.D. degrees in plasma engineering in 1987 and 1993, respectively, all from Seoul National University, Seoul, Korea.

He was with the Semiconductor Research Center, Hyundai Electronics, Seoul, Korea, from 1993 to 1995. Since 1995, he has been a Professor in the Department of Electrical Engineering, Inha University, Incheon, Korea. His research is currently focused on PDP.